Для підвищення ефективності неінвазивного моніторингу внутрішньої температури головного мозку здійснено розробку малогабаритного одноканального мікрохвильового радіотермографа, що складається з мініатюрного радіометра і радіометричного датчика на основі друкованої антени. Подібне рішення необхідно для того, щоб забезпечити лікарів системою неінвазивного бездозового моніторингу лікування та діагностики. В роботі описані математичне моделювання та експериментальна верифікація отриманих технічних рішень. Розроблено мініатюрний радіотермометрії, що є балансним модуляційним радіометром, побудованим на основі схеми R. H. Dicke з двома навантаженнями. З урахуванням вимог мініатюризації створений радіометричний датчик за допомогою чисельного моделювання. В результаті розрахунків визначено оптимальні розміри конструкції антени: загальний розмір ∅30 мм, розмір підкладки з фольгованого Флан склав – ∅23 мм, розмір щілини випромінювача – 16×2 мм. За даними математичного моделювання глибина виявлення теплових аномалій склала не менше 20 мм для друкованої антени, що практично не відрізняється від хвилеводної антени, яка успішно застосовується в радіотермометрії мозку.

Виконано вимірювання коефіцієнта стоячої хвилі для різних точок голови людини: лобової, скроневої, тім'яної, потиличної і перехідною між потиличної і тім'яної областями голови. Проведено експериментальні дослідження радіотермографи на водному фантомі і біологічному об'єкті. Показано дуже гарний збіг між даними чисельного моделювання та фізичного експерименту КСВ в діапазоні 1.04–1.8. В результаті досліджень встановлено, що радіотермограф з друкованою щілинною антеною дозволяє здійснювати вимірювання внутрішньої температури головного мозку з прийнятною точністю (±0.2 °С). Це забезпечить контроль краніоцеребральної гіпотермії мозку у пацієнтів з інсультом і дозволить оперативно змінювати тактику проведення гіпотермії. Невеликі розміри створеної апаратури дозволять поєднувати її з іншими медичними роботизованими системами для підвищення ефективності лікування

Ключові слова: мікрохвильова радіотермометрія, моніторинг температури, друкована антена, медичний радіотермограф, радіояскрава температура, медична робототехніка

UDC 182.536
DOI: 10.15587/1729-4061.2018.134130

DEVELOPMENT OF A MINIATURE MICROWAVE RADIOTHERMOGRAPH FOR MONITORING THE INTERNAL BRAIN TEMPERATURE

M. Sedankin
PhD, Researcher
Department of collection, processing and analysis of test results of robotic complexes, Main research and testing robotics centre of the Ministry of defence of the Russian Federation (MRTRC)
Seregina str., 5, Moscow, Russia, 125167
E-mail: msedankin@yandex.ru

D. Chupina
Department of Medical and technical information technologies
Bauman Moscow State Technical University
2-ya Baumanskaya str., 5, Moscow, Russia, 105005

S. Vesnin
PhD, Chief Designer
LLC "RTM Diagnostics»
Bol'shaya Pochtovaya str., 55/59,
Moscow, Russia, 105082

I. Nelin
PhD, Assistant professor
Department of Radiolocation, radio navigation and on-board radio electronic equipment
Moscow Aviation Institute
Volokolamskoe highway, 4,
Moscow, Russia, 125993

V. Skuratov
Engineer, Researcher
VNIIRT
Bol'shaya Pochtovaya, str., 22,
Moscow, Russia, 105082

1. Introduction

Cerebral crisis is a vital medical and social issue at present. Extending life span, population "aging" in developed countries, ever growing number of strokes among young people result in a growth of the general insult incidence. In the structure of mortality, acute cerebrovascular accidents occupy the second place after acute coronary pathology and make up about 19 % of the total mortality rate. About 6 million cases are recorded annually in the world. Cerebral stroke in Russian Federation annually affects about 500 thousand people or about 1.5 % of citizens more than

50 years old. Stroke leads to disability in 70–80 % of cases and a patient need for constant care in 20–30 % of cases [1–4].

Various diagnostic and treatment techniques including neuromonitoring in the course of treatment are required for stroke therapy. Existing high-tech radiological methods are too expensive, not always available and require highly qualified medical personnel. As the pathological changes of biological tissues are accompanied by a change in metabolism and tissue temperature, internal temperature can serve as an important diagnostic sign of various diseases. The known thermometric devices (infrared cameras, thermocouples, thermistors, liquid crystal films, flexible optical sensors, etc.) enable non-invasive temperature measurement of skin only. Magnetic resonance (MR) thermometry can be used to measure brain temperature [5] but this requires costly medical equipment, high-tech information technologies and additional scientific studies. In addition, the MR thermometry is unsuitable for the measurements repeated over a long period of time and still has a low accuracy of temperature measurement (>0.5 °C) [5–7].

Thermal methods conjugated with invasive procedures provide temperature information only for a definite region of the biological object (BO). In addition, they are very traumatic and are used only in emergencies. Non-invasive information on internal brain temperature can only be obtained with the help of microwave radiometry based on measuring the power of microwave brain radiation. Development of microwave radiometry as a method of neuromonitoring will make it possible to reveal various brain diseases, analyze dynamics of the brain state changes and control patient therapy and rehabilitation.

In order to effectively control treatment of brain diseases, it is necessary, first of all, to radically reduce the equipment size, both the RF channel and the device for information processing. Besides, new solutions are required in the field of small-size medical antennas which can be comfortably secured on the person's head. Because of a considerable size of the waveguide antennas available, it is impossible to secure them.

Today, internal BO temperature is measured mainly by means of waveguide antennas of circular and rectangular shape [15, 16]. These antennas are designed to work with the mammary gland and are not quite suitable for detection of brain pathologies. In addition to the waveguide antennas, the following types of antennas are widely used in medicine: frame (vibratory) [17], printed [18–20], and intracavitary [21] antennas. Due to the design simplicity, low cost and development of the technological level in the field of printed electronics, it is advisable to use printed antennas in brain examination. Unlike waveguide antennas, emitter in the printed antennas is applied directly on the dielectric substrate. In waveguide antennas, there is a section of the waveguide between the emitter and the aperture. Printed antennas are easier than waveguide antennas, cheaper and smaller and have less effect on the skin temperature. When designing, it is necessary to consider the fact that the printed antennas have higher electrical losses in the substrate than waveguide antennas. Printed antennas have become widespread in recent years. It is easier to fix the printed antenna on the patient's head and combine with other medical devices due to their small size if necessary. Therefore, development of a printed slot antenna is of relevance. According to [16], the antenna must receive the BO signal without reflections and be unsusceptible to radiation from the surrounding space. The antenna must also satisfy the following general requirements: acceptable harmonization with the BO in the working band of the radiometry and minimal impact on the BO temperature. The antenna design should have required noise immunity, good hygienic properties and low electrical losses. The printed antenna for examination of the mammary glands was considered in [16]. Thus, the second important step is a switch to the use of the printed antennas. To this end, it is necessary to adapt current technical solutions in the field of radiometry of mammary glands for their use in brain radiometry. Creation of a miniature device will enable effective, non-invasive measurement with an acceptable accuracy with no harm to the patient during a long time.

2. Literature review and problem statement

For the first time, radiometry in medicine was applied in the field of mammalology. Namely, the results of measurements of internal or brigthness or radiometric temperature (RT) in decimeter (λ=23 cm) and centimeter (λ=9 cm) ranges made for 1000 patients were presented in [8]. The results have shown a high sensitivity of radiometry in diagnostics of breast cancer. The works performed in [8] gave an impetus to scientific studies in the field of microwave radiometry around the world.

Today, several medical devices (single-channel and multichannel radiometers or radiothermographs) are known. They enable dynamic monitoring of the brain RT. MRTRS-40 multichannel radiothermographs for brain examination was developed by the Ecological and Medical Apparatus Design Bureau (Russia). A multichannel radiothermograph for brain examination was developed by Giperion LLC (Russia). A system for measuring brain temperature (Microwave Radiometry Imaging System, MiRaIS) was presented in [10]. However, it should be noted that most radiothermographs have large dimensions, even in a single-channel execution.

The MRTRS-40 system was used in [9] to measure brain self-radiation. The main technical characteristics of the system are as follows: the range of measured temperatures: 298–323 K; the range of measured frequencies: 650–850 MHz; fluctuation sensitivity: 0.05 K. The MRTRS-40 system has 3 non-invasive biomedical signal meters which simultaneously work in real time. This system features possibility of dynamic monitoring of internal brain temperature in several points simultaneously and analysis of the RT fluctuations. The examination is carried out in a special shielded cabin. The measurement results are displayed graphically as RT vs. time charts. The system has considerable dimensions and is suitable for stationary use only. It is quite difficult to combine it with other medical devices.

Information on development of a 20-channel microwave radiothermograph for visualizing thermal changes in brain was provided in [10]. This device has 20 input channels (antennas) and 2 operating ranges: 780 MHz and 1.5 GHz with a band of 200 MHz. The base of the device design is made of a mesh frame with U-shaped antennas evenly arranged in the frame which is fixed on the head surface. The device has adjustable straps which make it well adaptable to head shape and size. The radiometric sensor is realized on the basis of a U-shaped miniature vibrator antenna. Its design makes it possible to ensure good match with various parts of the patient's body. The results are visualized as a dynamic distribution of intensity of thermal radiation. The shielded

room must be used to operate the system. It enables quick readout from the head surface and formation of a picture of brain temperature fluctuation. This multichannel radiothermograph can only be used in a shielded room, it has significant dimensions and it is difficult to combine it with other medical devices.

The MiRaIS system is also used for brain examination [11]. The brain radiation readout is contactless within an elliptical cabin with conducting walls having a hole for the human head and representing an elliptical antenna with two focusing points. The receiving dipole antenna is located in the focusing point 1, and the BO is positioned in the focusing point 2. The MiRaIS system uses a RF receiver operating in four frequency ranges: 1.1 GHz, 1.8 GHz, 2.4 GHz and 2.8 GHz with a 150 MHz band in each range. The radiometer sensitivity is ±0.02 °C while sensitivity of the whole system is ±1 °C. The main disadvantage of the above devices [9–11] is that they do not possess a sufficient interference resistance and can only be used in special shielded cabins (capsules) which hampers their practical use.

The results of measurements of radiothermal brain radiation in the range of 3.2±0.45 GHz are given in [12]. A multichannel radiometer with a phased array was used. A printed conformal antenna with an emitter having an L-shaped slot was used as an array element. According to the authors, this system has limitations connected with accuracy and temperature resolution in comparison with other technologies. The proposed antenna system requires an additional study to determine its potential applicability in clinical practice.

Development of an anti-interference single-channel medical radiometer was presented in [13]. It is a hybrid device combining a microstrip receiving antenna based on a logarithmic spiral emitter and a main radiometer front-end. In other words, practically the whole radiometer, with the exception of some RF devices, is placed in the antenna housing which makes it possible to consider it as a miniature unit. The radiothermograph is based on a modified circuit of total power radiometer with two reference sources ("cold" and "hot"). The operating frequency of the unit is 1.35 GHz with a band of 500 MHz. The RF module is connected to the digital module containing additional amplifiers and filters. It has a USB cable for computer connection. Accuracy of the internal temperature measurement is ±0.4 °C. The unit was tested with various physical models of biological tissues: brown fat, kidneys, brain. This radiation thermometer can be considered as a miniature device but it is not built according to the R.H. Dicke's circuit and has considerable dimensions (the control unit measures 270×180 mm without antenna). These radiometers are still used for scientific purposes only and do not have a permission for medical use.

In current clinical practice, the method of craniocerebral hypothermia (CCH) is used. It helps to increase survival and reduce the adverse effects of cerebral disasters in patients. As the therapeutic effect of CCH is achieved by cooling the human head, it is necessary to control temperature in order to select the CCH tactics corresponding to the degree of brain damage [14]. The data obtained with the use of RTM-01-RES radiometer for monitoring cerebral CCH and studying thermal features of ischemic stroke make it possible to consider radiometry as a promising method for dynamic monitoring of patients with a stroke. The results obtained confirm onset of hyperthermia in the area of ischemic lesion. Because RTM-01-RES radiometer was developed for use in mammology, it is difficult to use it for dynamic monitoring of the state of biological tissues. As the unit has considerable dimensions, it is difficult to secure it on the patient's body. The antenna used in the RTM-01-RES radiometer was constructed on the basis of a round waveguide with considerable dimensions. The human's head surface is complex in shape with convexities and concavities, so it is difficult to fix this antenna on the head in the temperature measuring process and ensure a close fit. It is easier to attach a printed antenna to the patient's head and, if necessary, combine it with other medical devices due to its small size.

For brain examination, it is necessary to have small radiometric systems easily fixed on the patient's head for dynamic monitoring of microwave radiation. In the process of CCH, a neurohelmet with a refrigerant is fixed on the hairy part of the head according to the anatomy of brain to cool it. To control the brain cooling, it is enough to place a single-channel radiothermograph on free areas of the head (forehead, temple, etc.) to control cooling. Thus, clinical practice demands development of an antenna and a compact radiometer the design of which will enable effective application of the methods of radiometry and CCH simultaneously or alternately. In the future, inclusion of several antennas in a multichannel radiometer will make the CCH procedure more effective and provide doctors with a convenient multichannel device for brain examination.

Thus, there are no solutions at present that would enable creation of a miniature radiothermograph based on a balance radiometer with a printed slot antenna. The radiothermograph built according to the of R.H. Dicke's circuit is the only device ensuring high accuracy of measurements (<0.4 °C). Almost all modern radiometers are modifications of this radiometer [22–24]. The problem of developing an interference-free miniature radiometer is not solved so far which limits application of advanced technical solutions in medicine. In addition, equipment miniaturization will allow the device to be combined with robotic systems and improve quality of medical care as well as open up the prospects of dual use.

3. The aim and objectives of the study

This work objective was to develop a miniature radiothermograph for brain examination. To achieve this objective, the following tasks were solved:

– development of a miniature radiometer for brain examination;

– development of a miniature radiometric sensor based on a printed antenna;

– experimental verification of the obtained technical solutions.

4. The study materials and methods

4. 1. The basic principles of microwave radiometry

Biological tissues of the human body emit a noise signal with power related to RT (T_{rad}) as:

$$P = (1 - S_{11}^2) k_B T_{rad} \Delta f, \quad (1)$$

where k_B=1.38·10^{-23} J/K is the Boltzmann constant; Δf is the radiometer frequency band, GHz; S_{11} is the coefficient of reflection from the 'antenna – BO' interface.

By measuring the power of self-radiation, one can find the RT measured in the region under the antenna fixed on the body. The purpose of radiometric brain examination is to measure and visualize its RT. The measurements are carried out under the condition of a good electromechanical contact between the antenna and the head surface to ensure an acceptable match with the body. In most medical radiometers, the effect of the reflection coefficient on the measurement results is compensated, so S_{11}=0. Taking into account this fact, the RT will be determined by the following expression [15]:

$$T_{rad} = \int_{-\infty}^{\infty} T(r)W(r)dV, \quad (2)$$

where $T(r)$ is the BO physical real temperature, $W(r)$ is the radiometric weight function (RWF) of the antenna.

The RWF, W(r) is defined as:

$$W(r) = \frac{\frac{\sigma(r)}{2}\left(E(r)\right)^2}{\int_{-\infty}^{\infty} \frac{\sigma(r)}{2}\left(E(r)\right)^2 dV}, \quad (3)$$

where $E(r)$ is the intensity of the electric field (EF) generated by the antenna in the BO volume, and σ (r) is electrical conductivity of the BO tissue.

In the case of radiometry, the integral RT averaged over the volume with the weight function $W(r)$ is measured. It depends on the distribution of the antenna EF, $E(r)$ and the BO electrophysical parameters (ε(r), σ(r)).

To calculate distribution of EF, $E(r)$, numerical solution of the Maxwell equations is necessary for the BO model under study. To calculate physical temperature, $T(r)$, it is necessary to solve the equation of heat and mass transfer [21] taking into account the blood flow and biophysical parameters of the object under study. In the end, when these problems are solved, $T(r)$ and $E(r)$ can be found and the RT calculated. If temperature of the medium is constant and equal to T, then it follows from (2) that T_{rad}=T, that is, the RT and the physical temperature coincide. In other cases, the RT is equal to physical temperature averaged with the weight $W(r)$ in the volume of biological tissues under the antenna. That is, if the temperature $T(r)$ changes with the depth in the body, then equation (2) for the BO multilayer structure consisting of N layers is written as:

$$T_{rad} = \sum_{i=1}^{N} T_i \cdot C_i, \quad (4)$$

where C_i are weight coefficients for the multilayer structure, T_i is temperature of the i-th layer of the multilayer structure which characterize contribution of all BO layers to the measured RT.

Weight coefficients, Ci, are calculated as follows:

$$C_i = \frac{\frac{\sigma_i}{2}\int_{V_i}\left(\overline{E}(r)\right)^2 \mathrm{d}V}{\sum_{i=1}^{N}\frac{\sigma_i}{2}\int_{V_i}\left(\overline{E}(r)\right)^2 \mathrm{d}V}, \quad (5)$$

where V_i is the volume of the i-th layer of the multilayer structure.

If necessary, formulas (4) and (5) are used for final processing of the simulation data to determine weight coefficients and temperature of each layer. To calculate EF $E(r)$, it is necessary to carry out numerical modeling in the program of electrodynamic modeling taking into account electrical losses and the antenna design. Computations were performed using the HIPERCONE FDTD program [25] based on the EMTL (Electromagnetic Template Library) interface [26, 27]. The high-performance core of Hipercone uses a new class of asynchronous vectorized updates of the calculation grid. Its computational efficiency has reduced the calculation time several times compared to conventional FDTD programs. The program solves the Maxwell equations numerically taking into account the BO multilayer nature by the finite difference method in the time domain. The FDTD method enables analysis of interaction of an electromagnetic field with various objects and forms. Calculation is carried out in the following way. First, the countable domain (the volume in which the calculation is made) and the grid resolution (calculation step) are selected and boundary conditions specified. The body model with certain electrophysical properties is placed inside the countable domain. The program numerically solves the Maxwell equations in a finite-difference form with the values of the field components in each new step found using the values obtained in the previous steps. The initial conditions are set at t=0 (n=0): all values of the E and H fields are equal to zero in the whole countable domain. The components of tangential electric field are set to zero on conducting surfaces.

It is necessary to set initial values for all components of the domains that are determined by the excitation conditions. A slot vibrator is used as a system of excitation of electromagnetic waves in the antenna. Information on distribution of the antenna EF makes it possible to ascertain in what area the RT is measured, what dimensions it has and what is the contribution of various BO layers to it. To calculate the brain temperature rise in presence of pathology, it is necessary to calculate distribution of physical temperatures inside the head in presence and absence of a stroke. Thus, the study of the design of the antenna and calculation of its functional parameters and characteristics take place in two stages by the procedure detailed in [16]. First, the EF $E(r)$ is analyzed and then the real BO temperature and the RT are numerically calculated. For simplicity of analysis of the designed antenna, an increment of the RT (ΔT_{rad}) is usually calculated on the thermal anomaly projection and not the absolute temperature:

$$\Delta T_{rad} = \int_{-\infty}^{\infty} \Delta T(r)W(r)\mathrm{d}V. \quad (6)$$

The increment of thermodynamic temperature or thermoassymmetry, $\Delta T(r)$, is the difference in brain temperature in the presence of stroke ($T(r)$) and without it ($T_0(r)$):

$$\Delta T(r)=T(r)-T_0(r), \quad (7)$$

where $T(r)$ is the brain temperature in the presence of pathology, $T_0(r)$ is the brain temperature in absence of pathology.

Thus, the RT increment makes it possible to assess the possibility of diagnosing a concrete thermal anomaly with the help of the antenna being developed. In addition, it is possible to determine diagnostic possibilities of identifying a particular pathology by changing geometrical, thermophysi-

cal and electrophysical parameters of the mathematical model layers and the antenna geometry with the help of the unit.

4. 2. The miniature radiothermograph

A microwave radiothermograph typically includes three technical devices: a r adiometer, a radiometric sensor (antenna) and a control interface (microcomputer) with software. The radiometer is a high-sensitivity modulation receiver of ultralow electromagnetic radiation of the BO in a centimeter range. The device is intended for non-invasive measurement of the RT of the internal tissues of the BO, processing of SNF signals coming from the antenna and transmission of this information for visualization. In the course of this study, a miniature radiometer operating at a frequency of 3.6 GHz and having a bandwidth of 500 MHz has been developed.

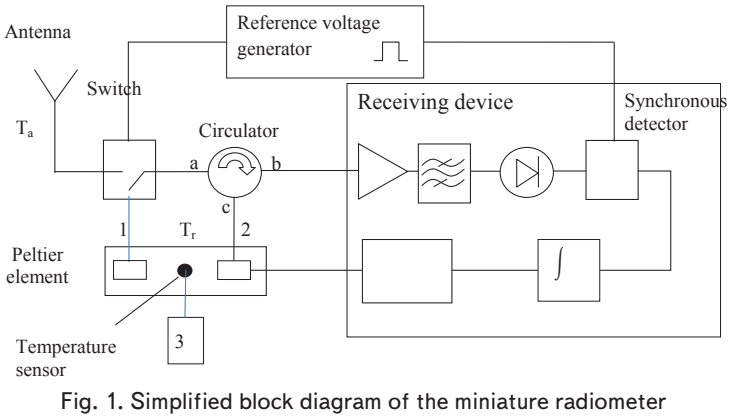

Fig. 1. Simplified block diagram of the miniature radiometer

The radiometer (Fig. 1) contains series connected antenna contacting with the BO, a switch, a circulator installed after the switch and a receiving device. Next, an amplitude detector, a narrowband low frequency amplifier, a synchronous detector, an integrator and a DC amplifier are sequentially installed in the receiving device. The reference voltage generator is connected to the switch and the synchronous detector. Also, the radiometer has two microwave loads installed on the Peltier element. The switch connects either the antenna or the load (1) (heated resistor) to the a-b arm of the circulator. The switch is controlled by a generator of reference voltage at a frequency of 1 kHz. The noise signal from the switch output passes through the circulator and enters the receiving device. In operation of this radiometer, voltage ΔU proportional to the difference between the noise temperature T_a coming from the antenna and the temperature T_r of the first heated resistor at the output of the receiving device is formed:

$$\Delta U = k_U (T_a - T_r), \quad (8)$$

where k_U is the coefficient of amplification of the receiving circuit of the radiometer.

This voltage is amplified and fed to the Peltier element. The temperature of the loads is measured using a contact temperature sensor that can be installed on the Peltier element or one of the loads. The temperature sensor has a tight thermal contact with the loads. The signal from the temperature sensor is integrated in an additional integrator, amplified and fed to an indicator or a computer (3) which performs the functions of the data processing and control unit. The second resistor unlocks the circulator from the input circuits of the low-noise amplifier, so this shoulder is match loaded. Structurally, the radiometer (Fig. 2) consists of two printed circuit boards with devices for processing RF and LF signals connected by a board-to-board connector. One board is the radiometer and the second board is the device for controlling its operation having a USB connector for computer connection.

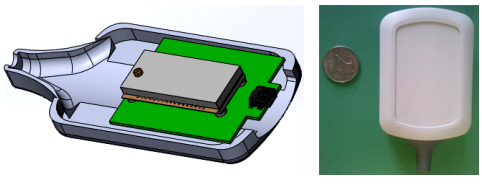

a *b*

Fig. 2. Miniature radiothermograph: the miniature radiometer (*a*); OKW Co. Connect case (*b*)

The entire radiometer is installed in the OKW Co. Connect case. This case has optimum ergonomic characteristics, dimensions suitable for the developed radiometer an adjustment option and is also conventionally used in medical devices. Overall dimensions of the radiometer: 76×54×22 mm.

4. 3. Miniature radiometric sensor

The radiometric sensor is of paramount importance for ensuring operation parameters of the radiometric since it determines diagnostic capabilities of the whole radiothermograph. The radiothermograph antenna fixed on the body surface serves as a sensor. To obtain an antenna, it should be designed with calculation of its EF. For calculations, a situation is modeled when the working surface of the antennas is in a direct contact with the BO. Let us consider a model of the antenna design shown in Fig. 3 used in calculations. The topology of the radiator in the form of a simple rectangular slot with dimensions of L×S [mm] is applied to the upper side of substrate with diameter D [mm] and thickness h [mm] with a dielectric constant ε. The lower open part of the substrate contacts with the BO.

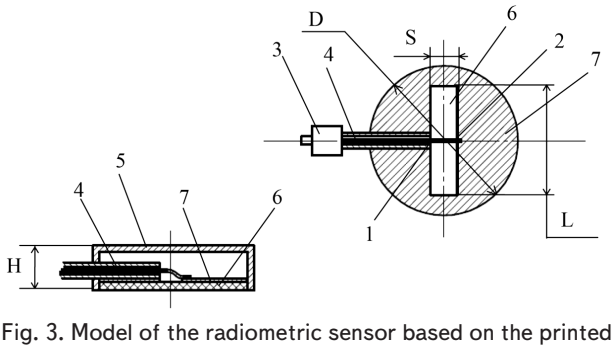

Fig. 3. Model of the radiometric sensor based on the printed antenna: coaxial cable soldering points (1, 2); RF connector (3); coaxial cable (4); the antenna housing (5); substrate (6), emitter (7)

In order to provide acceptable noise immunity, the substrate is installed in a metal housing with total height of H [mm]. The emitter is fed as follows: the outer conductor of the coaxial cable is soldered to one side of the slot and the internal conductor to the other side of the slot. The BO was modeled as a medium with large electrical losses (similar to the human head physical properties) and was a 100×100×100 mm multi-layered cube.

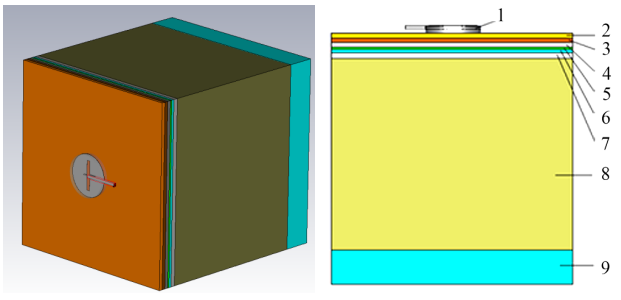

Fig. 4. The BO model: antenna (1); skin (2); fatty layer (3), bone tissue (4); pachymeninx (5); cerebrospinal fluid (6); gray matter (7); white matter (8); absorber (9)

The EF of the antenna was calculated for this BO volume. It was located in the center of the model at X_0=50 mm, Y_0=50 mm with radiation in the direction of the Z axis. The model of the BO with the antenna is shown in Fig. 4. The value of E_τ=0 was established at the model boundaries. The biophysical parameters of each BO layer in the 3.6 GHz frequency range are presented in Table 1.

Table 1

Electrophysical parameters of biological tissues in the 3.6 GHz range [15]

Electrophysical parameters / Biological tissue	Dielectric constant, ε	Electrical conductivity, σ ([S/m])	Thickness of the biological tissue layer, mm
Skin	36.920	2.086	2
Fat layer	5.164	0.160	2
Cranium bones	5.176	0.152	2
Pachymeninx	40.593	2.439	1
Cerebrospinal fluid	64.410	4.691	1.5
Gray matter	47.159	2.720	2.5
White matter	34.897	1.873	84

The electrodynamic simulation program was used to calculate the antenna EF. It solves the Maxwell equation for a multilayer medium with losses taking into account the antenna design by the method of finite differences in the time domain. A slot vibrator in the form of a simple rectangular slot was used as a system of excitation of electromagnetic waves in the antenna.

Imaginary and actual values of the EF E (x, y, z) components of the antenna in the BO medium were calculated. The program allows one to obtain data on the reflection coefficient and other S-parameters of the antenna and carry out its primary analysis. To select optimal geometric dimensions of the antenna design and the substrate material, mathematical modeling was performed with variation of geometric parameters of the antenna. In optimization, RWF and the standing wave ratio (SWR) were used as performance criteria. The antenna design should minimize mismatch (S_{11}) between the antenna and the BO. SWR and S_{11} are related as:

$$SWR = \frac{1+|S_{11}|}{1-|S_{11}|}. \quad (9)$$

RWF depends on the EF distribution which is commonly used in analysis of transmitting antennas. However, taking into account the principle of reciprocity of properties of antennas for transmission and reception, it is permissible to use this parameter when analyzing antennas. RWF and its parameters are very vivid for comparison of various variants of the designed antenna. The most important parameters and characteristics of antennas are RWF, resolving power, dimensions and shape of the measurement area of the RT, depth of measurement, increase in the RT on the projection of the thermal anomaly, ΔT_{rad} [16]. RWF and the RT measurement range enable interpreting the maximum RT measurement depth as an optimality criterion. SWR control makes it possible to minimize power reflections from the BO. Electrical parameters and characteristics of medical antennas determine diagnostic capabilities.

5. Results of the mathematical modeling of the printed antenna

A number of calculations of variants of the printed antenna design were performed in the course of theoretical studies. The parameters (D, ε, H, h, L, S) of the antenna shown in Fig. 3 were used as the initial parameters for simulation. These parameters were used to optimize the antenna geometry during mathematical modeling. The antenna is placed in a metal case with outside diameter D+2=25 mm and height H=5 mm.

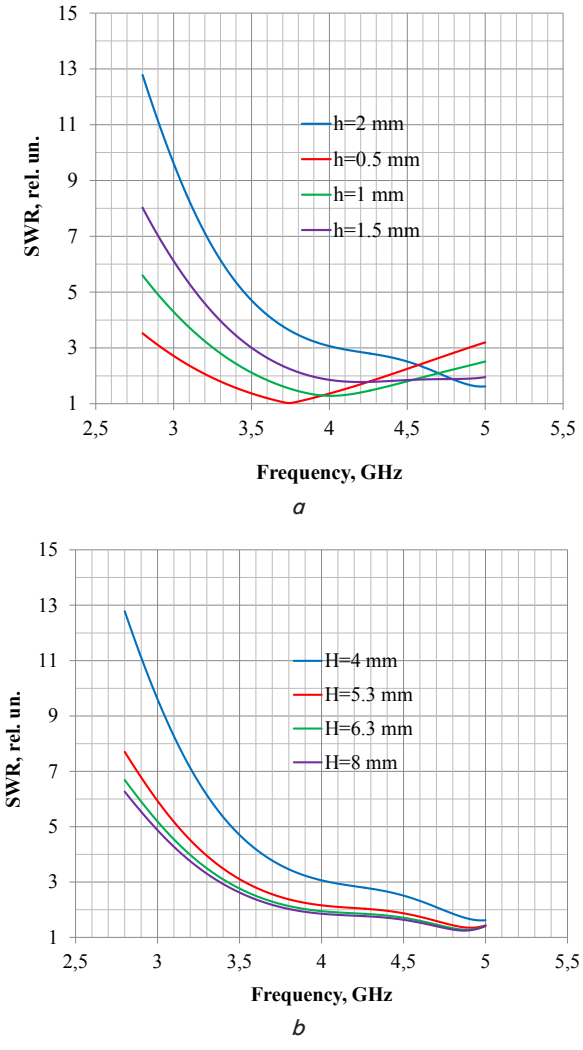

Fig. 5. SWR of the printed antenna at various parameters: h=0.5; 1; 1.5 [mm] (*a*); H=4; 5.3; 6.3; 8 [mm] (*b*)

The antenna substrate with diameter D=23 mm was placed inside the case, the relative dielectric constant of the substrate ε=20, thickness *h*=1.5 mm. The emitter slot measured 16×2 [mm].

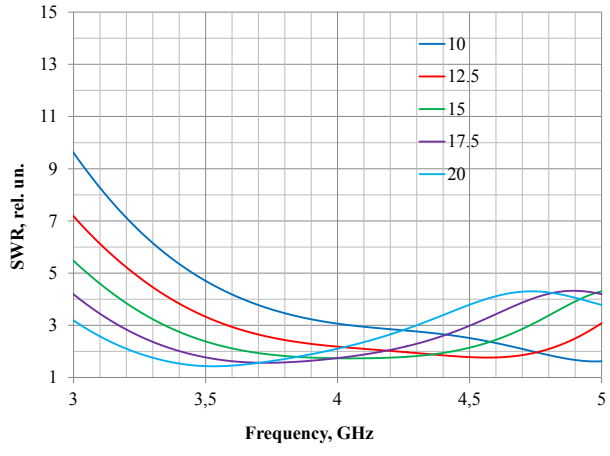

a

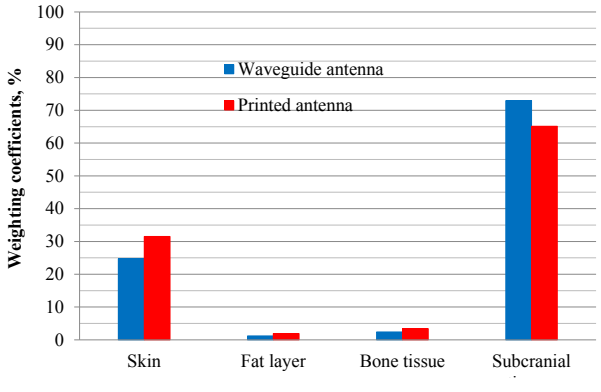

b

Fig. 6. Calculations results: dependence of SWR on frequency at various values of dielectric constant ε=10; 12.5; 15; 17.5; 20 (*a*); weight coefficients for the waveguide antennas and printed antennas (*b*)

The calculations were carried out with variation of any one antenna parameter and with invariance of the rest. The following parameters were varied: thickness, *h*, dielectric constant, ε, of the substrate, total height, *H*, of the antenna, parameters of the emitter slot, *L*×*S*, etc., the antenna impedance in the working frequency band was analyzed in the Volpert-Smith diagram. Diameter and height of the antenna were chosen after consultation with doctors. The first series of calculations related to the *h* parameter variation. The calculations were performed at *h*=0.5; 1; 1.5; 2 [mm] with other antenna parameters unchanged. SWR at various substrate thicknesses, *h*, are presented in Fig. 4.

Further, calculation was made with variation of the antenna body height: *H*=4; 5.3; 6.3; 8 [mm]. The remaining parameters were constant and *h*=2 mm. The optimum result was obtained at *H*=5.3 mm (Fig. 5, *b*). Further calculations were carried out at *H*=5.3 mm, *h*=2 mm and at unchanged initial parameters with variation of the dielectric constant ε=10; 12.5; 15; 17.5; 20. The results are presented in Fig. 6, *a*. As can be seen from Fig. 5, 6, the printed antenna had an acceptable matching in the selected frequency range. Then, the results of calculation of a waveguide antenna (Ø32 mm) which has already been successfully used in treatment of brain stroke [22] are given for comparison. In accordance with formula (5), contribution of skin to the measured RT was determined (Fig. 6, *b*) for two antennas. Also, calculation of the RT in which 85 % of the power measured by the antenna was focused. The RT measurement areas for two antennas in the E and H planes are shown in Fig. 7, 8.

According to the calculation results, the measurement depth (the measurement area length in the *Z* axis) was 20 mm for both antennas. For the waveguide antenna, the width of the measurement area was 60.7 mm in the *X*-axis and 36 mm in the *Y* axis (Fig. 7). For the printed antenna, the width of the measurement area was 73.4 mm in the *X* axis and 28 mm in the *Y* axis (Fig. 8). According to the calculation results, it is obvious that the selected antenna variant meets requirements of microwave radiometry [16] and has quite acceptable characteristics and parameters.

According to data from [15], the temperature increase in the presence of stroke is determined from formulae (10) and (11):

$$T(r)=A\cdot e^{\frac{-r^2}{\left(B\frac{D}{2}\right)^2}}, \tag{10}$$

$$r^2=(x-x_0)^2+(y-y_0)^2+(z-z_0)^2, \tag{11}$$

where *x*, *y*, *z* are the current coordinates; x_0, y_0, z_0 are the coordinates of the location center; *D* is the affected zone diameter; *A*, *B* are the approximation coefficients for 3 stroke cases: *A*=1.15, *B*=0.95 (core: Ø10 mm, envelope: Ø20 mm); *A*=1.88, *B*=0.9 (core: Ø15 mm, envelope: Ø30 mm) and *A*=2.47, *B*=0.85 (core: Ø20 mm, envelope: Ø40 mm).

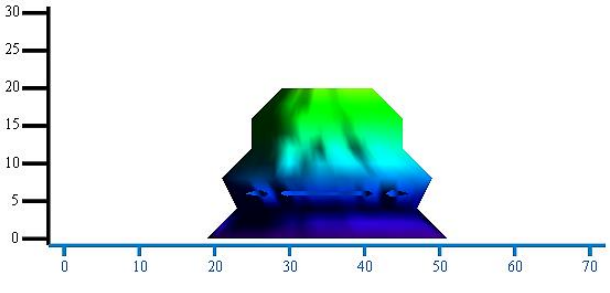

a

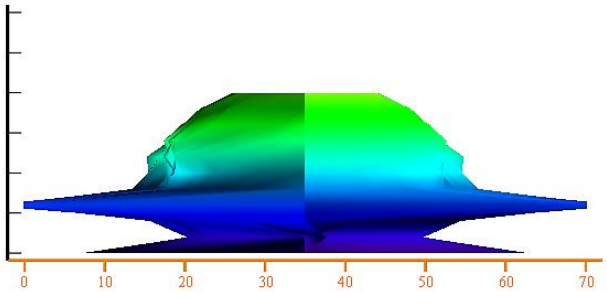

b

Fig. 7. The volume under investigation of the waveguide antenna measurement (3.6 GHz): the *XZ* plane (*a*), the *YZ* plane (*b*)

Further, in accordance with expression (7), calculation of RT was performed on the projection of three cases of brain stroke for waveguide and printed antennas. Fig. 9 shows

dependence of ΔT_{rad} on diameter of the stroke and the depth of its location. Thus, according to the calculations, it can be concluded that the microwave radiometer is capable of detecting thermal changes within the brain in the presence of ischemic stroke regardless of the antennas used: printed or waveguide. Although the printed antenna records slightly lower values of the RT increase, nevertheless, the differences are negligible. Thus, characteristics of the printed and waveguide antennas practically do not differ in their work with the brain.

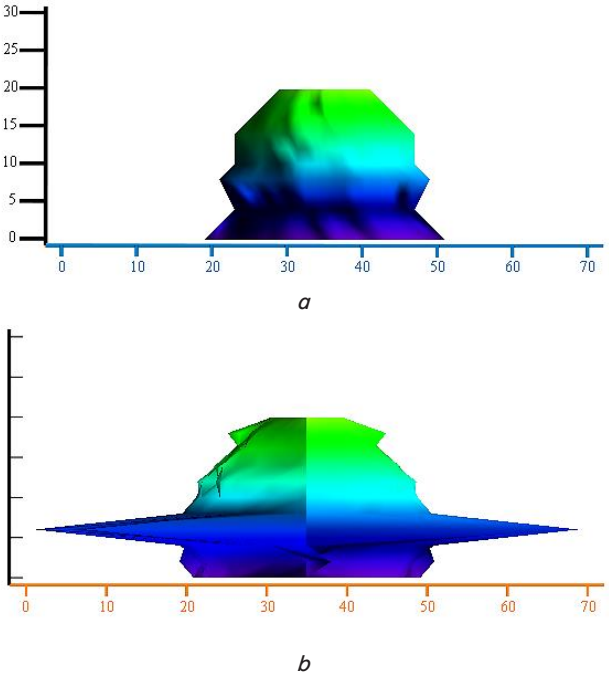

a

b

Fig. 8. The volume under investigation of the printed antenna measurement (3.6 GHz): the *XZ* plane (*a*), the *YZ* plane (*b*)

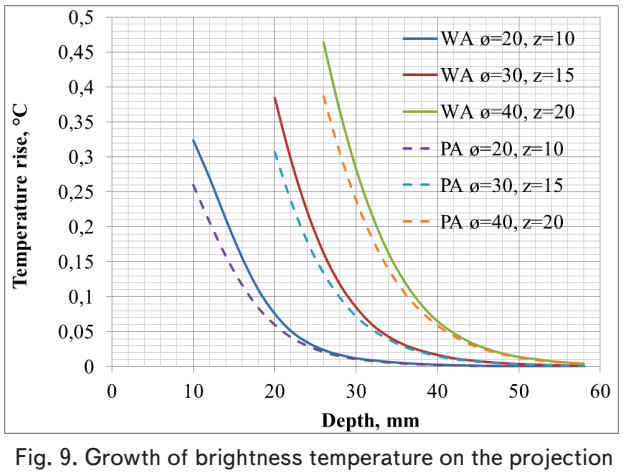

Fig. 9. Growth of brightness temperature on the projection of stroke for 3 cases: waveguide antenna (WA), printed antenna (PA)

6. Experimental studies of the printed antenna efficiency

The most successful and ergonomic solution is embodiment in the form of a drop-shaped body with overall dimensions Ø30×5 [mm] (Fig. 10). There is a board with a digital temperature sensor in the lower part of the antenna to monitor the antenna body temperature during thermal compensation. The signal from the antenna is fed to the radiometer via a coaxial cable. The optimal geometric dimensions of the antenna: Ø30 mm, diameter of the foil-clad flan substrate was 23 mm, the emitter slot dimensions: 16×2 mm. Electrical parameters of the substrate: dielectric constant ε=10, loss tangent tg=$1 \cdot 10^{-4}$.

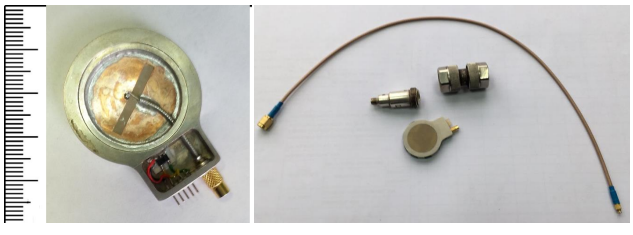

a *b*

Fig. 10. Manufacture and verification of a radiometric sensor: printed antenna (*a*); devices for experimental studies (*b*)

The total height of the antenna was 5 mm. The SWR of antennas was measured by the Micran R2M-04 module meter of coefficients of transmission and reflection in the frequency range 0.01...4.0 GHz. This is the range of the SWR meter. Conventionally, when working in the 0.6 GHz frequency band, measurements are carried out in a wider band. The wider the band the better in terms of ease of use since the obtained characteristic can be frequency shifted up or down. The results of measurements are shown in Fig. 11 where the SWR characteristics are presented in the 3.4...4.0 GHz band when the antenna was fixed to the frontal, temporal, parietal, occipital head regions and the transition part between the occipital and parietal regions.

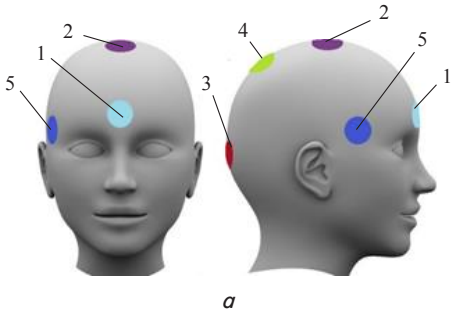

a

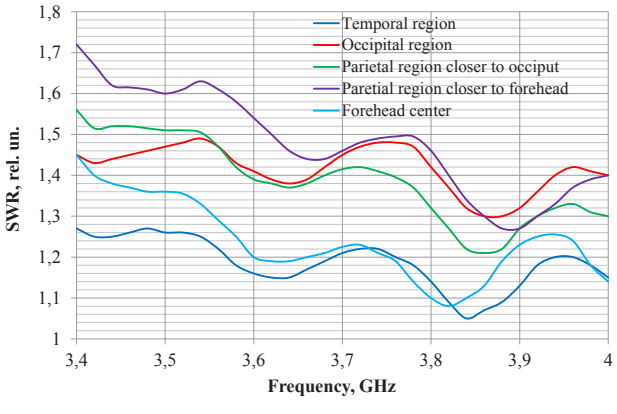

b

Fig. 11. Measurement of SWR in various points on human head: the points of SWR measurement (*a*); the results of SWR measurement in various points (*b*)

It is worth noting that the best results of the antenna matching were achieved when working in the central part of the forehead and in the temporal region. Somewhat worse results were obtained when the antenna worked in the parietal region. Taking into account the physiological features of structure of the skull bones, one can conclude that the best results were obtained in the most even head regions. In these regions, a uniform contact of the antenna plane with the head and a larger quantity of soft tissues take place. In the regions such as the parietal region where curvature of the skull bone is the greatest, the antenna readings of SWR were somewhat worse because of uneven contact of the antenna with the head surface. Nevertheless, the results were quite acceptable in all cases, i. e. SWR≤2. The designed radiometer is based on a balance radiometer according to the R.H. Dicke's circuit. This radiometer compensates for the mismatch with the BO (SWR≤2), therefore the developed radiometric sensor is optimal for use in the radiometer. Fig. 12, *b* shows the results of numerical simulation and experimental measurements for comparison, and Fig. 12, *a* shows general appearance of the single-channel radiothermograph.

In order to show acceptable sensitivity of the unit, water temperature in two thermostats was measured at various temperatures in accordance with the standard antenna calibration adopted in radiometry. The antenna was kept in the thermostat for several minutes at water temperature T=32 °C, then it was quickly moved to another thermostat with water temperature T=38 °C. The experimental bench and the results of water temperature measurements are presented in Fig. 12, *c, d*. It is obvious that a successful compact antenna design was obtained with good matching and expected thermal characteristics.

7. Discussion of the results obtained in the study of a miniature radiothermograph

Description of the studies related to the development of a single-channel miniature radiometer is presented in this work. This unit can be used for rapid long-term monitoring of the RT from a depth of several centimeters in the range of 3.4–4.2 GHz. Long-term monitoring of brain is characteristic for CCN, open heart surgery or carotid arteries with their short-term forcipressure. At present, there is no compact neuromonitoring system in medicine enabling noninvasive real-time acquisition of information on internal brain temperature. Such unit development was based on the design of a miniature balance radiometer with two loads and a radiometric sensor based on a printed slot antenna.

a

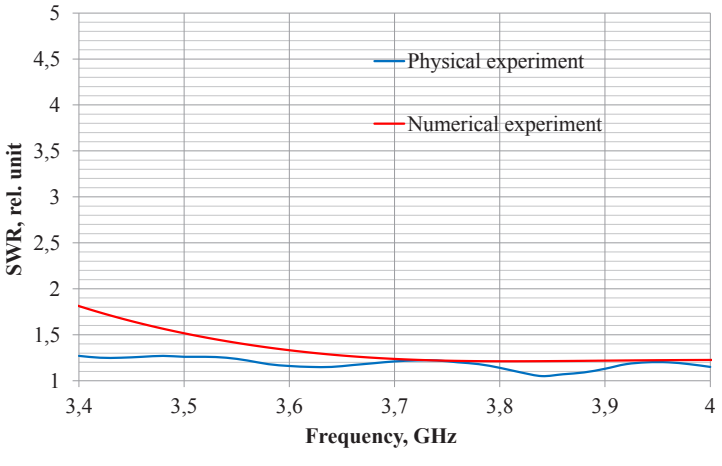

b

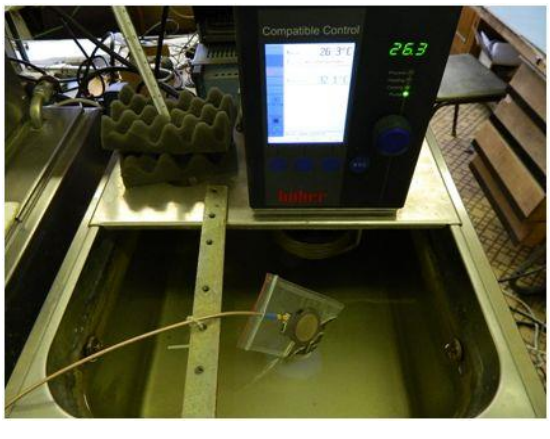

c

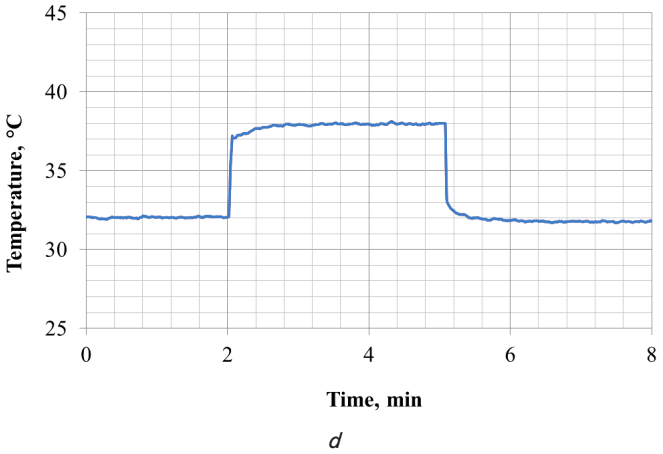

d

Fig. 12. The radiometric system and its experimental data: appearance of the single-channel radiothermograph (*a*); comparison of data obtained in numerical and physical experiments (patient) (*b*); experimental bench (water phantom) (*c*); the measurement results (water phantom) (*d*)

In order to understand the diagnostic possibilities of radiometry in relation to brain stroke, a mathematical modeling of its own microwave radiation was performed taking into account the antenna design. The printed slot antenna is a key element of the whole radiometer. Effectiveness of brain radiometry was estimated using numerical simulation and experimental studies. Design and operating frequency of the antenna were optimized using numerical simulation with the following criteria: maximizing the power taken by the antenna from the brain tissues in comparison with other tissues; maximizing the bandwidth of the antenna and the impedance corresponding to the tissue (SWR≤2). Electrodynamic simulation has demonstrated the possibility of efficient recording of thermal radiation to detect temperature rise caused by pathology at a depth of 20 mm. Pathological foci located deeper than 20 cm can also be detected by the unit due to heat transfer.

A series of experimental studies of measuring SWR in five head points was performed with Micran R2M-04 meter. A very good coincidence of numerical simulation and physical experiment (SWR in the range 1.04–1.8) was obtained. The sensor was made as a light, drop-shaped noise-protected body which can be held in place by a special tape or elastic belt. It was shown that this type of the radiothermograph design ensures stable recording of internal brain temperature. It is clear from Fig. 12 that the results of RT measurement coincide with a high accuracy (±0.2 °C) with the results of measurement of water temperature by means of a precision mercury thermometer. The greatest divergence of the results was observed at the moment of immersion of the antenna in water. This is explained by the fact that the antenna temperature at the beginning of measurement affected the obtained results. At the moment of immersion, the antenna temperature differed from the water temperature, so the measurement results differed from the thermostatically controlled water temperature until the antenna reached the water temperature.

It has also been shown that the unit can be used for non-invasive monitoring of functional brain activity, even though it does not provide temperature data, like magnetic resonance thermometry. Fig. 12, *d* shows coincidence of the results of measurement of the water phantom temperature and the results of measurement with a precision mercury thermometer at two temperatures (32 °C and 38 °C). The unit can also be used for monitoring CCH to decide on the best tactics of the brain stroke treatment. The study results were used in development of a miniature single-channel radiothermograph for brain examination.

The limitation of this device consists in that the single-channel device enables temperature monitoring in just one point. Consequently, monitoring will be based on the analysis of the RT dynamics in time which is suitable for long-term thermal monitoring of functional activity of some brain regions.

For the further work, it is planned to upgrade the technology by means of using radiometric sensors based on metallized textile materials and flexible silicon-like dielectric materials. This will ensure the most even contact of the antenna plane with the head surface. In general, a successful compact design of a single-channel radiothermograph is available at present. It has an acceptable match of the printed antenna with the expected thermal characteristics. Development and application of a printed antenna in medicine will make it possible to use radiometry to diagnosticate various brain diseases. Practical realization of the study results will consist in a creation of innovative products and incorporation of radiometric devices into medical robotic complexes, etc. Moreover, the knowledge of actual brain temperature will help to reduce the number of complications and, consequently, the total cost of surgery for improving clinical outcomes for the patients receiving pre- and postoperative CCH.

8. Conclusions

1. It has been established that there are several technical solutions in the field of single-channel and multichannel radiothermographers for brain examination. To use such systems, special screened rooms are required. Most of the devices are of considerable dimensions and are suitable only for stationary use. It is also impossible to integrate these devices with other medical devices and those being the part of the wearable technologies. Creation of a miniature device will enable effective, non-invasive RT measurement with an acceptable accuracy and for a long time.

2. The study has resulted in development of a single-channel contact radiothermograph with a printed antenna for receiving microwave brain radiation in a range of 3.6 GHz with a band of 500 MHz. The balance radiometer designed on the basis of the R.H Dicke's circuit was chosen as the electric circuit for the radiometer. This radiothermograph can be operated in non-shielded rooms.

3. The results of biomedical verification of the technical solutions have confirmed that the system performed the specified functions. A stable temperature record with an error of ±0.2 °C was ensured and the SWR does not exceed 2 for various head points. Considering that the balance radiometer compensates for the mismatch with the SWR not more than 2, the diagnostic system acceptable for medical practice was obtained. Based on mathematical modeling, it was shown that the method makes it possible to diagnose thermal anomalies of the cerebral cortex of large brain hemispheres. Due to the thermal conductivity from deep layers, the device is capable of detecting thermal anomalies located much deeper (Fig. 9).

4. Based on the results of mathematical modeling (SWR<2, measurement depth of 20 mm, contribution of subcranial brain tissues of ≈70 %, bandwidth of ≈500 MHz), an optimal design was chosen and a radiometric sensor based on the printed slot antenna was made. The antenna was made in the form of a drop-shaped body with overall dimensions of Ø30×5 [mm]. The radiometer with the printed antenna has shown sensitivity sufficient to monitor internal BO temperature for a potential record of clinically significant measurement results with an accuracy of ±0.2 °C.

References

1. Starodubceva O. S., Begicheva S. V. Analiz zabolevaemosti insul'tom s ispol'zovaniem informacionnyh tekhnologiy // Medicinskie nauki. Fundamental'nye issledovaniya. 2012. Issue 8. P. 424–427.

2. Global and regional burden of stroke during 1990–2010: findings from the Global Burden of Disease Study 2010 / Feigin V. L., Forouzanfar M. H., Krishnamurthi R., Mensah G. A., Connor M., Bennett D. A. et. al. // The Lancet. 2014. Vol. 383, Issue 9913. P. 245–255. doi: 10.1016/s0140-6736(13)61953-4
3. Gusev E. I. Problema insul'ta v Rossii // Zhurnal nevrologii i psihiatrii. 2003. Issue 3. P. 3–10.
4. Kraniocerebral'naya gipotermiya kak perspektivniy metod neyroprotekcii na dogospital'nom etape okazaniya medicinskoy pomoshchi / Lisickiy V. N., Kalenova I. E., Boyarincev V. V., Pas'ko V. G., Bazarova M. B., Sharinova I. A. // Kremlevskaya medicina. Klinicheskiy vestnik. 2013. Issue 2. P. 197–202.
5. Magnetic resonance thermometry: Methodology, pitfalls and practical solutions / Winter L., Oberacker E., Paul K., Ji Y., Oezerdem C., Ghadjar P. et. al. // International Journal of Hyperthermia. 2015. Vol. 32, Issue 1. P. 63–75. doi: 10.3109/02656736.2015.1108462
6. MR safety: FastT1thermometry of the RF-induced heating of medical devices / Gensler D., Fidler F., Ehses P., Warmuth M., Reiter T., Düring M. et. al. // Magnetic Resonance in Medicine. 2012. Vol. 68, Issue 5. P. 1593–1599. doi: 10.1002/mrm.24171
7. Accuracy of real time noninvasive temperature measurements using magnetic resonance thermal imaging in patients treated for high grade extremity soft tissue sarcomas / Craciunescu O. I., Stauffer P. R., Soher B. J., Wyatt C. R., Arabe O., Maccarini P. et. al. // Medical Physics. 2009. Vol. 36, Issue 11. P. 4848–4858. doi: 10.1118/1.3227506
8. Barrett A., Myers P. Subcutaneous temperatures: a method of noninvasive sensing // Science. 1975. Vol. 190, Issue 4215. P. 669–671. doi: 10.1126/science.1188361
9. Kublanov V. S., Borisov V. I., Dolganov A. Yu. Primenenie mul'tifraktal'nogo formalizma pri issledovanii roli vegetativnoy regulyacii v formirovanii sobstvennogo elektromagnitnogo izlucheniya golovnogo mozga // Medicinskaya tekhnika. 2016. Issue 1. P. 21–24.
10. Prognozirovanie kachestva i nadezhnosti IS SVCh na etapah razrabotki i proizvodstva / Leushin V. Yu., Gudkov A. G., Korolev A. V., Leushin V. Yu., Plyushchev V. A., Popov V. V., Sidorov I. A. // Mashinostroitel'. 2014. Issue 6. P. 38–46.
11. Noninvasive Focused Monitoring and Irradiation of Head Tissue Phantoms at Microwave Frequencies / Karathanasis K. T., Gouzouasis I. A., Karanasiou I. S., Giamalaki M. I., Stratakos G., Uzunoglu N. K. // IEEE Transactions on Information Technology in Biomedicine. 2010. Vol. 14, Issue 3. P. 657–663. doi: 10.1109/titb.2010.2040749
12. Asimakis N. P., Karanasiou I. S., Uzunoglu N. K. Non-invasive microwave radiometric system for intracranial applications: a study using the conformal l-notch microstrip patch antenna // Progress In Electromagnetics Research. 2011. Vol. 117. P. 83–101. doi: 10.2528/pier10122208
13. Stauffer P. R., Rodrigues D. B., Maccarini P. F. Utility of microwave radiometry for diagnostic and therapeutic applications of non-invasive temperature monitoring // 2014 IEEE Benjamin Franklin Symposium on Microwave and Antenna Sub-systems for Radar, Telecommunications, and Biomedical Applications (BenMAS). 2014. doi: 10.1109/benmas.2014.7529480
14. Diagnosticheskie vozmozhnosti neinvazivnogo termomonitoringa golovnogo mozga / Cheboksarov D. V., Butrov A. V., Shevelev O. A., Amcheslavskiy V. G., Pulina N. N., Buntina M. A., Sokolov I. M. // Anesteziologiya i reanimatologiya. 2015. Issue 1. P. 66–69.
15. Vesnin S. G., Sedankin M. K., Pashkova N. A. Matematicheskoe modelirovanie sobstvennogo izlucheniya golovnogo mozga cheloveka v mikrovolnovom diapazone // Biomedicinskaya radioelektronika. 2015. Issue 3. P. 17–32.
16. Sedankin M. K. Antenny-applikatory dlya radiotermometricheskogo issledovaniya teplovyh poley vnutrennih tkaney biologicheskogo ob'ekta: diss. ... kand. tekhn. nauk. Moscow, 2013. 247 p.
17. A novel design of thermal anomaly for mammary gland tumor phantom for microwave radiometer / Lee J.-W., Kim K.-S., Lee S.-M., Eom S.-J., Troitsky R. V. // IEEE Transactions on Biomedical Engineering. 2002. Vol. 49, Issue 7. P. 694–699. doi: 10.1109/tbme.2002.1010853
18. Bardati F., Iudicello S. Modeling the Visibility of Breast Malignancy by a Microwave Radiometer // IEEE Transactions on Biomedical Engineering. 2008. Vol. 55, Issue 1. P. 214–221. doi: 10.1109/tbme.2007.899354
19. Temperature Measurement by Microwave Radiometry: Application to Microwave Sintering / Beaucamp-Ricard C., Dubois L., Vaucher S., Cresson P.-Y., Lasri T., Pribetich J. // IEEE Transactions on Instrumentation and Measurement. 2009. Vol. 58, Issue 5. P. 1712–1719. doi: 10.1109/tim.2008.2009189
20. Jacobsen S., Rolfsnes H. O., Stauffer P. R. Characteristics of Microstrip Muscle-Loaded Single-Arm Archimedean Spiral Antennas as Investigated by FDTD Numerical Computations // IEEE Transactions on Biomedical Engineering. 2005. Vol. 52, Issue 2. P. 321–330. doi: 10.1109/tbme.2004.840502
21. Sedankin M. K., Novov A. A., Abidulin E. R. Trekhkanal'naya mikrovolnovaya antenna dlya urologii // Mezhdunarodnaya nauchno-tekhnicheskaya konferenciya «Informatika i tekhnologii. Innovacionnye tekhnologii v promyshlennosti i informatike». Moscow, 2017. P. 289–291.
22. Design of small-sized and low-cost front end to medical microwave radiometer / Klemetsen O., Birkelund Y., Maccarini P. F., Stauffer P., Jacobsen S. K. // Prog Electromagn Res Symp. 2010. P. 932–936.
23. Dicke R. H. The Measurement of Thermal Radiation at Microwave Frequencies // Review of Scientific Instruments. 1946. Vol. 17, Issue 7. P. 268–275. doi: 10.1063/1.1770483
24. Vaysblat A. V. Medicinskiy radiotermometr // Biomedicinskie tekhnologii i radioelektronika. 2001. Issue 8. P. 3–9.
25. Using memory-efficient algorithm for large-scale time-domain modeling of surface plasmon polaritons propagation in organic light emitting diodes / Zakirov A., Belousov S., Valuev I., Levchenko V., Perepelkina A., Zempo Y. // Journal of Physics: Conference Series. 2017. Vol. 905. P. 012030. doi: 10.1088/1742-6596/905/1/012030
26. Creating Numerically Efficient FDTD Simulations Using Generic C++ Programming / Valuev I., Deinega A., Knizhnik A., Potapkin B. // Lecture Notes in Computer Science. 2007. P. 213–226. doi: 10.1007/978-3-540-74484-9_19
27. FDTD subcell graphene model beyond the thin-film approximation / Valuev I., Belousov S., Bogdanova M., Kotov O., Lozovik Y. // Applied Physics A. 2016. Vol. 123, Issue 1. doi: 10.1007/s00339-016-0635-1